KfK 5166
März 1993

General Corrosion and Stress Corrosion Cracking Studies on Carbon Steels for Application in Nuclear Waste Disposal Containers

E. Smailos, B. Fiehn, J. A. Gago, I. Azkarate
Institut für Nukleare Entsorgungstechnik

Kernforschungszentrum Karlsruhe

Kernforschungszentrum Karlsruhe
Institut für Nukleare Entsorgungstechnik

KfK 5166

GENERAL CORROSION AND STRESS CORROSION CRACKING STUDIES ON CARBON STEELS FOR APPLICATION IN NUCLEAR WASTE DISPOSAL CONTAINERS

E. Smailos, B. Fiehn, J.A. Gago *, I. Azkarate **

* ENRESA, Spain
** INASMET, Spain

Annual report 1992 prepared within the framework of the 1991-1994 programme of the European Atomic Energy Community: "Management and storage of radioactive waste". Task 3: Characterization and qualification of waste forms, packages and their environment. EC-Research Contract No. FI2W-CT90-0030.

Kernforschungszentrum Karlsruhe GmbH, Karlsruhe

Kernforschungszentrum Karlsruhe GmbH
Postfach 3640, 7500 Karlsruhe 1

ISSN 0303-4003

Summary

In previous corrosion studies, carbon steels and the alloy Ti 99.8-Pd were identified as promising materials for heat-generating nuclear waste containers acting as a radionuclide barrier in a rock salt repository. To characterize the long-term corrosion behaviour of these materials in more detail, a research programme including laboratory-scale and in-situ corrosion studies has been undertaken jointly by KfK and ENRESA/INASMET. Besides carbon steels and Ti 99.8-Pd, also Hastelloy C4 and some selected Fe-base materials are being examined in order to complete the results available to date.

In the period under review, the 18-month immersion experiments and the stress corrosion cracking studies (slow strain rate tests) on three preselected carbon steels in disposal relevant brines at 150°C-170 °C were completed. Moreover, first irradiation-corrosion studies were performed on the unalloyed carbon steel TSt E 355 in salt brines at 150°C and a realistic gamma dose rate of 10 Gy/h for thick-walled containers.

The corrosion results obtained from the 18-month immersion tests are in good agreement with previous findings for up to 1 year. They confirm that the low-alloyed steels TStE 460 and 15 MnNi 6.3 are subjected to general corrosion in the brines, and that the linear corrosion rates (56-71µm/a in NaCl-rich brine, 65-203µm/a in $MgCl_2$-rich brines) imply corrosion allowances acceptable for a thick-walled container. For the submerged arc welded (SAW) steel specimens, simulating a potential container closure technique, however, severe local corrosion attacks were detected for both steels in the heat-affected zone after testing in the $MgCl_2$-rich brines at 150°C. The results obtained from the 100-day experiments under gamma irradiation indicate that a dose rate of 10Gy/h does not diminish the resistance of the unalloyed steel TStE 355 to pitting corrosion in the brine, and that the corrosion rates (21µm/a NaCl-rich brine, 173-208µm/a in $MgCl_2$-rich brines) are reasonable for the corrosion allowance container concept discussed.

In the slow strain rate tests at 170°C and 10^{-4} - 10^{-7} s^{-1}, a loss of ductility occurred for the steels in an $MgCl_2$-rich brine compared to argon. This was probably due to hydrogen embrittlement. However, this effect is not significant and no indication for stress corrosion cracking was found for the hot-rolled steels TStE 355 and TStE 460. On the contrary, the forged steel 15 MnNi 6.3 was susceptible to stress corrosion cracking at rates of 10^{-5} s^{-1} and 10^{-6} s^{-1}. Further laboratory-scale and in-situ corrosion studies are in progress.

Untersuchungen zur Flächen- und Spannungsrißkorrosion von Stählen als Werkstoff für Behälter zur Endlagerung radioaktiver Abfälle

Zusammenfassung

Bisherige Korrosionsuntersuchungen ergaben, daß Kohlenstoffstähle und die Legierung Ti 99.8-Pd aussichtsreiche Materialien für langzeitbeständige Behälter zur Endlagerung von wärmeerzeugenden Abfällen in Steinsalzformationen sind. Zur detaillierten Charakterisierung des Korrosionsverhaltens dieser Werkstoffe werden von KfK und ENRESA/INASMET in einem gemeinsamen Forschungsprogramm weitergehende Untersuchungen durchgeführt. Neben Stählen und Ti 99.8-Pd werden zur Vervollständigung der bisher vorliegenden Ergebnisse auch Hastelloy C4 und einige ausgewählte Eisenbasiswerkstoffe untersucht.

Im Berichtszeitraum wurden die 18-Monats-Immersionsexperimente und die Spannungsrißkorrosionsuntersuchungen bei langsamen Dehnungsraten an drei ausgewählten Stählen in endlagerrelevanten Salzlösungen bei 150°C-170°C abgeschlossen. Darüber hinaus wurden erste Korrosionsexperimente (100 Tage) an dem unlegierten Stahl TStE 355 in Salzlösungen bei hoher Temperatur (150°C) und einem realistischen Gamma-Strahlenfeld für dickwandige Behälter von 10Gy/h durchgeführt.

Die Korrosionsergebnisse an den niedriglegierten Stählen TStE 460 und 15 MnNi 6.3 nach 18 Monaten Immersion in den drei Salzlösungen (eine NaCl-reich, zwei $MgCl_2$-reich) bei 150°C sind in guter Übereinstimmung mit den Ergebnissen bisheriger Untersuchungen bis zu 1 Jahr. Sie bestätigen, daß die Grundwerkstoffe beständig gegenüber Lochkorrosion sind und daß die linearen Raten der Flächenkorrosion (56-71µm/a in der NaCl-reichen Lösung bzw. 65-203µm/a in den $MgCl_2$-reichen Lösungen) zu technisch akzeptablen Korrosionszuschlägen für einen dickwandigen Behälter führen. Auch die unterpulvergeschweißten Stahlproben (Simulation einer möglichen Behälterverschlußtechnik) blieben nach 18 Monaten Prüfzeit in der NaCl-reichen Lösung beständig gegenüber Lochkorrosion. In den $MgCl_2$-reichen Lösungen hingegen wurden bei den 18-Monats-Schweißproben, wie in den bisherigen Untersuchungen, starke lokale Korrosionsangriffe in der Wärmeeinflußzone festgestellt. Die bisherigen Ergebnisse der Korrosionsuntersuchungen unter Gammabestrahlung zeigen, daß eine Dosisleistung von 10 Gy/h die Beständigkeit des Stahls TStE 355 in Salzlösungen gegenüber Lochkorrosion nicht herabsetzt und daß die Korrosionsraten (21µm/a in der NaCl-reichen Lösung, 173-208µm/a in den $MgCl_2$-reichen Lösungen) zu realistischen Behälterwandstärken führen.

In den Korrosionsuntersuchungen in einer $MgCl_2$-reichen Lösung bei 170°C und Dehnungsraten von 10^{-4} - 10^{-7} s^{-1} nahm die Duktilität der Stähle gegenüber Argon deutlich ab, was möglicherweise auf eine H_2-Versprödung zurückzuführen ist. Allerdings war dieser Effekt nicht signifikant und es waren keine Anzeichen für eine Spannungsrißkorrosion bei den warmgewalzten Stählen TStE 355 und TStE 460 festzustellen. Der Schmiedestahl 15 MnNi 6.3 hingegen zeigte in der Lösung bei Dehnungsraten von 10^{-5} s^{-1} und 10^{-6} s^{-1} eine Anfälligkeit gegenüber Spannungsrißkorrosion. Weitere Labor- und in situ-Korrosionsuntersuchungen sind im Gange.

Table of contents

1. INTRODUCTION AND OBJECTIVES

According to the German concept, the heat-generating nuclear waste such as vitrified high-level waste and spent fuel will be disposed of in repositories located in deep rock-salt formations. The isolation of the radionuclides from the biosphere shall be ensured by a combination of geological and engineered barriers. One element of this multi-barrier concept is the waste packaging. Consequently, studies have been undertaken by KfK within the framework of the European Community research programme to develop long-term resistant packagings that act as a barrier during the elevated-temperature phase in the disposal area which lasts for a few hundred years. For this purpose, packaging materials with long-term corrosion resistance in rock salt and salt brines must be identified. Salt brines in the disposal area may originate from the thermal migration of brine inclusions in the rock salt and have to be considered in accident scenarios, e.g., brine inflow through an anhydride layer.

In previous corrosion studies [e.g. 1,2], carbon steels and the titanium alloy Ti 99.8-Pd were identified as the most promising materials for the manufacturing of long-lived containers surrounding the Cr-Ni steel waste canisters. To characterize the corrosion behaviour of these materials in more detail, a 1991-1994 EC research programme is being performed jointly by KfK and ENRESA/INASMET (Spain). Three carbon steels, which are discussed in Germany as container materials for the disposal of spent fuel, are the subject of investigations. These are: The unalloyed fine-grained steel TStE 355 and the low-alloyed steels TSt E 460 and 15 MnNi 6.3.

The research programme consists of two parts. The KfK part is aimed at studying the influence of important parameters on the long-term corrosion behaviour of the preselected carbon steels and Ti 99.8-Pd in disposal relevant salt brines. These parameters are: Temperature, gamma radiation and selected characteristics of packaging manufacturing. Both laboratory-scale immersion experiments and in-situ corrosion studies at the Asse salt mine are being carried out. Besides carbon steels and Ti 99.8-Pd, also Hastelloy C4 and the Fe-base materials, nodular cast iron, Ni-resist D2 and Ni-resist D4, are being examined in the in-situ corrosion experiments in order to complete the results available to date.

The second part of the corrosion studies concerns the investigation of the resistance of the carbon steels to stress corrosion cracking in a disposal relevant

salt brine at various strain rates and temperatures by ENRESA/INASMET. For this purpose, the slow strain rate technique (SSRT) is applied. These studies serve to complete the results available so far on statically loaded U-bend specimens. The entire research programme is coordinated by KfK.

In the period under review, the long-term general and local corrosion experiments, and the stress corrosion cracking studies on the steels in brines at 150°C - 170°C were completed. Moreover, first corrosion experiments lasting 100 days were performed on the unalloyed steel TStE 355 in brines at high temperature (150°C) and a realistic gamma radiation field of 10Gy/h (10^3 rad/h) for the thick-walled containers discussed.

2. MATERIALS AND SPECIMENS

The three carbon steels investigated in brines had the following compositions (wt.%):

Fine-grained steel TStE 355 (unalloyed):
0.17 C; 0.44 Si; 1.49 Mn; bal. Fe

TSt E 460 (low-alloyed):
0.18 C; 0.34 Si; 1.5 Mn; 0.51 Ni; 0.15 V; bal. Fe

15 MnNi 6.3 (low-alloyed):
0.17 C; 0.22 Si; 1.59 Mn; 0.79 Ni; bal. Fe

The parent materials of TStE 355 and TStE 460 were hot-rolled and annealed plates, and for 15 MnNi 6.3 forged and annealed disks. For the steels TStE 355 and TStE 460, a ferritic microstructure with perlite bands typical of the rolling process was observed. A grain size value of 10 according to ASTM E- 112 was measured for both steels. For the forged steel 15 MnNi 6.3, a ferrite-perlite microstructure of a duplex grain size with an average value of 9 (according to ASTM E- 112) was observed.

For the investigation of the general and local corrosion in brines, plane specimens of the dimensions 40mm x 20mm x 4mm were used. Prior to specimen fabrication, the parent materials were freed from the adhering oxide layer by milling. After this mechanical treatment, the specimens were cut and cleaned with alcohol in an ultrasonic bath.

The steel TStE 355 was examined for general and local corrosion in the brines in the as-received condition only. In case of the steels TStE 460 and 15 MnNi 6.3, submerged arc welded (SAW) specimens were tested in addition to specimens of the parent materials with a view to examine the influence of this welding technique discussed for the spent fuel disposal container closure on the corrosion. For the welding of the steels, materials in the forged and annealed condition were used.

For the stress corrosion cracking experiments (slow strain rate tests), round specimens of 6 mm diameter were machined and finished with 1000 grade emery paper. The TStE 355 and TStE 460 steels were machined in the transverse sense to the rolling direction of the plates, those of 15 MnNi 6.3 in the radial direction of the forged disks. In addition to the parent materials, also stress corrosion cracking studies were performed on MAG (Metal Active Gas) welded materials simulating an alternative container closure technique to SAW. The filler materials used for the welding were Griduct SV-8 for the unalloyed steel TStE 355 and Thyssen Union K-5Ni for the low-alloyed steels TStE 460 and 15 MnNi 6.3. Submerged arc welded (SAW) specimens were not investigated because the results obtained from the general and local corrosion studies (see section 3.4.1) have shown that this welding technique significantly reduces the corrosion resistance of the steels in $MgCl_2$-rich brines.

3. GENERAL AND LOCAL CORROSION TESTING OF CARBON STEELS IN BRINES WITH AND WITHOUT GAMMA IRRADIATION

3.1 Test conditions

In order to have severe test conditions, the steels were investigated under conditions simulating an accident with an intrusion of large amounts of brine into the disposal area. To examine the influence of the brine composition on the corrosion behaviour of the steels, three disposal relevant salt brines differing qualitatively and quantitatively were used as corrosion media. Two of them, brine 1 (Q-brine) and brine 2, were highly concentrated in $MgCl_2$, the third one (brine 3) had a high concentration of NaCl. The compositions and the measured pH and O_2-values of the test brines are given in Table I. The pH values given are relative data and were measured using a glass electrode. Application of the correction formula proposed by Bates et al. [3] gives pH values at 25°C which are

higher than the measured values by 1.8-2.2 units for brines 1 and 2, and by 0.4 units for brine 3. The O_2 values of the brines were determined by a polarographic method using an O_2 sensor; the saturation values (1.0-1.4mg O_2/l) obtained by the Winkler method were used as the reference values.

For up to 18 months, the low-alloyed steels TSt 460 and 15 MnNi 6.3 were examined for general and local corrosion in the brines up to 18 months at a temperature of 150°C that roughly corresponds to the maximum temperature on the surface of the disposal containers according to the German concept. The experiments were performed without gamma irradiation, because the dose rate expected on the surface of the about 30cm thick walled spent fuel disposal containers discussed is negligibly low. Corresponding studies on the unalloyed steel TStE 355 without irradiation were reported in previous work [4]. However, by using carbon steel containers for disposal of vitrified high-level waste (HLW) in boreholes, mechanical and corrosion allowances of the order of 10-15cm are discussed for containers with a service life of 300 years. In this case, gamma dose rates of 1 Gy/h - 10 Gy/h are calculated. To get information about the influence of gamma radiation on the corrosion of the steels at high temperature, the unalloyed fine-grained steel TStT 355 was tested for 100 days in the brines at 150°C in the presence of a gamma irradiation of 10 Gy/h. Experiments under gamma irradiation of up to 18 months are in progress. Investigations under gamma irradiation are important because the radiolytic products formed by the effect of radiation on salt brines, e.g., H_2O_2, ClO^- ,ClO_3^- etc. [5], might influence the corrosion process.

3.2 Experimental

For the corrosion experiments without irradiation, stainless steel pressure vessels provided with corrosion resistant insert vessels made of PTFE were used in order to avoid evaporation of the brines (boiling point: About 115°C). Into these vessels the brines were filled and the specimens immersed. After the pressure vessels had been closed, they were stored in heating chambers at 150°C. The experiments were performed at an equilibrium pressure of 0.4 MPa. To determine the corrosion kinetics, specimens were examined at various immersion times (maximum 18 months).

The corrosion experiments under gamma irradiation were performed in the spent fuel storage pool of KFA Jülich. The radiation source were spent fuel elements with a gamma energy spectrum similar to that of 10-year-old vitrified HLWC [2]. The experimental setup is shown schematically in Fig.1. For the experiments, autoclaves made of the corrosion resistant alloy Ti 99.8-Pd with insert vessels of Duran glass were used. The autoclaves were placed in a circular configuration in heated cylindrical stainless steel containers (irradiation containers).

For irradiation the containers were positioned at the bottom of the 6 m deep water-filled spent fuel element storage pool. The specimens and corrosion media were heated to the test temperature of 150°C using heaters.

3.3 Post-test examination of the specimens

When the specified test duration has been achieved, the specimens were removed from the brines and treated according to the ASTM guidelines. For this, the specimens were freed from the adhering salts and corrosion products by cleaning in distilled H_2O at 60°C and pickling in the Clark solution (37% HCl + Sb_2O_3 + $SnCl_2$) with subsequent cleaning in distilled H_2O and alcohol. After drying, the specimens were examined for general and local corrosion. General corrosion was calculated from the gravimetrically determined integral weight losses and the material density. The examination for local corrosion was made by microscopic evaluation, measurements of pit depth, surface profilometry and metallography. Additional information on the corrosion mechanism was obtained from the analysis of the corrosion products by means of X-ray diffraction (XRD).

3.4 Results

3.4.1 Corrosion of the low-alloyed steels TStE 460 and 15 MnNi 6.3 in brines without gamma irradiation

The general corrosion of the unwelded 18-month steel specimens (parent materials) at 150°C in the three brines, expressed as the thickness reduction, is plotted in Fig.2. For comparison, also the results of previous studies [6] of up to 12 months duration have been entered. The corrosion results obtained for the 18-month specimens made of TStE 460 and 15 MnNi 6.3 agree well with those of up to 12 months. They confirm that the thickness reduction of the steels increases

linearly with exposure time, i.e., the linear corrosion rate is time independent. The values of the linear corrosion rates of the steels are compiled in Table II. The lowest corrosion rates occurred in the NaCl-rich brine 3 with values of 56 µm/a (TStE 460) and 71 µm/a (15 MnNi 6.3), respectively. In the $MgCl_2$-rich brines 1 (Q-brine) and 2, higher corrosion rates (65-203µm/a for TStE 460, 94-117µm/a for 15 MnNi 6.3) were obtained compared to the values of the NaCl-rich brine. The higher corrosivity of the $MgCl_2$-rich brines compared to the NaCl-rich brine is attributed to their higher HCl-concentration. This could be explained by the higher Cl^- - concentration and the hydrolysis of Mg^{2+}. The acceleration of steel corrosion in brines containing high amounts of $MgCl_2$ is in line with the results reported by Westerman et al. [7].

It is evident from the metallographic examinations and the surface profiles that the unwelded 18-month specimens were resistant to pitting corrosion in all three brines. A non-uniform corrosion was observed for both steels in the test brines which is attributed to inhomogeneities of the steel composition. However, the maximum penetration depth of this uneven corrosion attack corresponded to the values of the average thickness reduction. Characteristic optical micrographs of the steels TStE460 and 15MnNi 6.3 after an 18-month exposure to brine 1 (Q-brine) at 150°C are shown in Fig. 3.

Welding did not influence noticeably the corrosion behaviour of the steels in the NaCl-rich brine 3. The SAW specimens underwent a non-uniform corrosion attack as did the unwelded specimens, and the general corrosion rates corresponded to the values obtained for the parent materials. In the $MgCl_2$-rich brines, however, considerable local corrosion attacks were detected for both steels in the heat-affected zone. The depth of these corrosion attacks increased with exposure time to the brines and after 18 months reached values between 2 mm and 4 mm, depending on the steel and the brine (Tab.III). Fig.4 shows optical micrographs of welded specimens of the steels TStE 460 and 15 MnNi 6.3 after an 18-month exposure to brine 1.

The corrosion products formed on the surface of the steel specimens were analysed by X-ray diffraction. For specimens exposed to the NaCl-rich brine 3, Fe_3O_4 (magnetite) and γ-Fe_2O_3 (maghemite) were identified. In the $MgCl_2$-rich brines, $(Fe, Mg)(OH)_2$ of the amakinite structure and β-FeOOH (akaganeite) were found, with no evidence of oxides. The formation of Fe_3O_4 and $(Fe, Mg)(OH)_2$ in

NaCl-rich and $MgCl_2$-rich brines, respectively, is also reported by Westerman et al. [7].

3.4.2 Corrosion of the unalloyed steel TStE 355 in brines with gamma irradiation

Specimens of the unalloyed steel TStE 355 were investigated for 100 days in the three brines given in Table I at a temperature of 150°C and a gamma dose rate of 10 Gy/h. The integral corrosion rates of the specimens calculated from the weight losses and the material density are compiled in Table IV. All values are average of three specimens. In the $MgCl_2$-rich brines 1 and 2, significantly higher general corrosion rates of 173µm/a and 208µm/a, respectively, were determined than in the NaCl-rich brine 3 (21µm/a), as in previous investigations without irradiation [4].

Surface profiles and metallographic examinations of corroded specimens have shown that the steel was resistant to pitting corrosion in all irradiated brines. After the test time of 100 days, a non-uniform general corrosion was observed in the $MgCl_2$-rich brines. However, the measured maximum penetration depth of this uneven corrosion corresponded to the value of the average thickness reduction. In case of the NaCl-rich brine, the corrosion attack of the steel specimens was fairly uniform. Figure 5 shows optical micrographs of steel specimens after 100 days of exposure to the test brines at 150°C and 10Gy/h.

In general, it can be stated that the corrosion rates determined so far for the steel under gamma irradiation imply corrosion allowances technically acceptable for the thick-walled containers discussed. For a final statement regarding the influence of gamma radiation on the corrosion of carbon steels in brines at the high temperature of 150°C, the results of the ongoing long-term experiments are necessary.

4. STRESS CORROSION CRACKING TESTING OF CARBON STEELS IN BRINES

4.1 Experimental

The resistance of the three preselected carbon steels TStE 355, TStE 460 and 15MnNi 6.3 to stress corrosion cracking was examined in the $MgCl_2$-rich brine 1

(Q-brine) by means of the slow strain rate technique (SSRT). The compositions of the steels and the brine are given in Session 2 and in Table I, respectively.

The experiments on the parent materials and MAG (Metal Active Gas) welded specimens were performed in Hastelloy C-276 autoclaves at strain rates of 10^{-4} - 10^{-7} s^{-1}, a temperature of 170°C, and an argon pressure of 13MPa. In order to be able to interpret the results obtained in the brine, additional comparative investigations were carried out in argon as an inert medium. Corresponding stress corrosion cracking studies on the steels at lower temperatures of 25°C and 90°C are in progress.

For the experiments, the round specimens (6 mm in diameter) were located in the Hastelloy C-276 autoclaves and attached to a fixed frame by one end and to the pull rod by the other. Fittings made of ZrO_2 ensured the electrical insulation of the specimens. Then the autoclaves were filled either with brine or argon, closed, pressurized and heated. Once the testing temperature and pressure were reached, the specimens were pulled until fracture at the selected actuator displacement speed.

Load, position, time and temperature data were continuously logged by the microprocessor controlling the testing machine. After each test, the elongation (E), reduction of area (R.A.), energy, yield strength (Y.S.), maximum load, and true stress at fracture were calculated. To evaluate the resistance of the steels to stress corrosion cracking, metallographic and scanning electron microscopic (SEM) examinations of the fracture specimen surfaces were performed in addition to the tensile experiments.

4.2 Results

The results of the slow strain rate tests obtained for the three steels in argon and Q-brine at 170°C and a strain rate of 10^{-7} s^{-1} are given in Figs. 6 and 7. For comparison, also the values at strain rates of 10^{-4} s^{-1}, 10^{-5} s^{-1} and 10^{-6} s^{-1} obtained in previous work [6] are plotted. All values are averages of at least two tests. Compared to the values in argon, a clear decrease in the elongation, reduction of area, energy and true stress at fracture occurred for all steels in the brine. This finding is in agreement with the results reported by Westerman et al. [7]. The

values for the yield strength and maximum load in Q-brine, however, are very close to those obtained in argon.

The metallographic examinations of specimens made of the hot-rolled steels TStE 355 and TStE 460 have shown that after testing in Q-brine at strain rates of $10^{-4}s^{-1}$ -10^{-6} s^{-1}, a non-uniform general corrosion occurred due to repeated breaking of the corrosion surface layer. At the lowest strain rate of 10^{-7} s^{-1}, the corrosion attack in the brine was fairly uniform. Figure 8 shows optical micrographs of the steel specimens tested in Q-brine at 170°C and a strain rate of 10^{-5} s^{-1}. Secondary cracks typical for stress corrosion cracking were not observed. For this reason, the reduction in ductility of the steels in Q-brine compared to argon cannot be attributed to stress corrosion cracking. For the loss of ductility in this brine another mechanism such as embrittlement could be responsible.

In the SEM examinations of TStE 355 and TStE 460 specimens tested in argon, a ductile fracture was observed at all strain rates. In Q-brine, the morphology of the fracture specimen surface depended on the strain rate. At 10^{-4} s^{-1} a beginning embrittlement, at 10^{-5} s^{-1} and 10^{-6} s^{-1} small brittle features at the specimen edges, and at 10^{-7} s^{-1} an embrittlement of larger specimen areas were observed. Figure 9 shows SEM micrographs of TStE 355 and TStE 460 after testing in Q-brine at 170°C and strain rates of 10^{-5} s^{-1} and $10^{-7}s^{-1}$, respectively.

In the metallographic examinations of the forged steel 15 MnNi 6.3 tested in Q-brine at strain rates of 10^{-4} s^{-1} and 10^{-7} s^{-1}, no secondary cracks indicating stress corrosion cracking were observed. On the contrary, at strain rates of 10^{-6} s^{-1} and particularly 10^{-5} s^{-1}, a clear susceptibility to stress corrosion was observed. Besides a non-uniform corrosion, extensive lateral secondary cracks were identified (Fig.10). The results of the SEM examinations are very similar to those of the steels TStE 355 and TStE 460. In Q-brine at 10^{-4} s^{-1}, only negligible embrittlement, and at 10^{-5} s^{-1} -$10^{-7}s^{-1}$ a brittle fracture of larger specimen areas was observed. In argon, the fracture surface was ductile. The SEM micrograph in Fig. 11 shows the brittle fracture of a 15 MnNi 6.3 steel specimen tested in Q-brine at 170°C and a strain rate of 10^{-5} s^{-1}.

The embrittlement of the steels in Q-brine at 170°C and slow strain rates is probably due to the hydrogen produced during corrosion which enters the materials in the atomic form, predominantly in zones of high stress level, and causes a loss of ductility. However, this effect does not appear to be serious

because the residual reduction of area and elongation at fracture of the steels after testing in the brine environment are still relatively high.

The results obtained for the MAG-welded steel specimens in argon and in Q-brine at 170°C and strain rates of 10^{-4} s^{-1} - 10^{-7} s^{-1} are plotted in Figs.12-13. Welding caused only a slight decrease of the elongation, reduction of area and energy compared to the values of the parent materials (Figs. 6-7). Moreover, the reduction of these properties in Q-brine compared to argon was very similar to that observed for the parent materials. Metallographic and fractographic studies of welded specimens are in progress.

5. CONCLUSIONS

In salt brines relevant for a rock salt repository, the low-alloyed steels TStE 460 and 15 MnNi 6.3 are resistant to pitting corrosion and the linear rates of general corrosion at 150°C (56 -71µm/a in NaCl -brine, 65-203µm/a in $MgCl_2$-rich brines) imply corrosion allowances acceptable for thick-walled containers. Submerged arc welding (SAW) does not influence the corrosion behaviour of the steels in NaCl - brine. In $MgCl_2$-rich brines, however, severe local corrosion attacks in the heat-affected zone of the SAW specimens were observed. Thus, the application of this welding technique is not recommended for the container closure.

First results of irradiation - corrosion studies in salt brines at 150°C indicate that a gamma dose rate of 10 Gy/h does not diminish the resistance of the unalloyed steel TStE 355 to pitting corrosion, and that the corrosion rates are reasonable for the corrosion allowance container concept discussed.

Slow strain rates of 10^{-4} -10^{-7} s^{-1} reduce the ductility of the steels TStE 355, TStE 460 and 15 MnNi 6.3 in $MgCl_2$-rich brine at 170°C compared to argon which is likely due to hydrogen embrittlement. However, this effect does not appear to be serious and does not cause stress corrosion cracking for the hot -rolled steels TStE 355 and TStE 460. On the contrary, the forged steel 15 MnNi 6.3 is susceptible to stress corrosion cracking in this brine at rates of 10^{-5} s^{-1} and 10^{-6} s^{-1}. Metal active gas (MAG) welded steels exhibit a very similar corrosion behaviour to the parent materials in the brine.

Further laboratory-scale and in-situ corrosion studies on carbon steels, Ti 99.8-Pd and Hastelloy C4 with and without gamma irradiation are in progress.

ACKNOWLEDGMENTS

The authors thank Prof. Dr. Jae Il Kim for reviewing this paper, Mrs. R. Weiler and Mr. P. Donath for preparing the optical micrographs and the X-ray diagrams, and the Commission of the European Communities, Brussels, Belgium, for supporting this work.

6. REFERENCES

[1] E. Smailos, "Korrosionsuntersuchungen an ausgewählten Werkstoffen als Behältermaterial für die Endlagerung von hochradioaktiven Abfallprodukten in Steinsalzformationen", KfK 3953 (1985).

[2] E. Smailos, W. Schwarzkopf, R. Köster et al., "Corrosion Testing of Selected Packaging Materials for Disposal of High-Level Waste Glass in Rock Salt Formations", KfK 4723 (1990).

[3] R.G. Bates, B.R. Staples, and R.A. Robinson, "Ionic Hydration and Single Ion Activities in Unassociated Chlorides at High Ionic Strength," Analytical Chemistry 42, 8, 867 (1970).

[4] E. Smailos, and R. Köster, "Corrosion of HLW Packaging Materials in Disposal Relevant Salt Brines," Proc. of the Int. Conf. on High-Level Radioactive Waste Management," Las Vegas, Nevada, USA, April 12-16, 1992, Vol. 2, 1992, p. 1676.

[5] G.H. Jenks, "Radiolysis and Hydrolysis in Salt-Mine Brines," ORNL/TM-3717, Oak Ridge National Laboratory (1972).

[6] E. Smailos, W. Schwarzkopf, I.A. Gago, and I. Azkarate, "Corrosion Studies on Selected Packaging Materials for Disposal of Heat-Generating Radioactive Wastes in Rock Salt Formations," KfK 5011 (1992).

[7] R.E. Westerman, J.H. Haberman et al.; " Corrosion and Environmental-Mechanical Characterization of Iron-Base Nuclear Waste Package Structural Barrier Materials", PNL Report No. 5426 (1986)

Table I: Compositions, pH values and O_2 contents of the salt brines used in the laboratory - scale corrosion experiments

Brine	Composition (wt.%)							
	NaCl	KCl	$MgCl_2$	$MgSO_4$	$CaCl_2$	$CaSO_4$	K_2SO_4	H_2O
1	1.4	4.7	26.8	1.4	---	---	---	65.7
2	0.31	0.11	33.03	---	2.25	0.005	---	64.3
3	25.9	---	---	0.16	---	0.21	0.23	73.5

pH (25°C): 4.6 for brine 1; 4.1 for brine 2; 6.5 for brine 3
O_2(55°C): 0.8 mg/l for brine 1; 0.6 mg/l for brine 2; 1.2mg/l for brine 3

Table II: Linear corrosion rates of the unwelded steels TST E 460 and 15 MnNi 6.3 in the test brines at 150°C

Material	Corrosion rate (µm/a)		
	Brine 1	Brine 2	Brine 3
TStE 460	203.5	65.4	56.3
15 MnNi 6.3	117.3	94.0	71.3

brines 1 and 2: $MgCl_2$ - rich; brine 3: NaCl - rich
test duration: 18 months

Table III: Maximum penetration depth of corrosion in the HAZ[+)] of the submerged arc welded steels TStE460 and 15 MnNi 6.3 after 18 months of exposure to brines at 150°C

Material	Maximum penetration depth (mm)		
	Brine 1	Brine 2	Brine 3
TStE 460	2.0	2.5	0.04
15 MnNi 6.3	1.9	4.0	0.05

[+)] heat - affected zone

Table IV: Integral corrosion rates of the unalloyed steel TStE 355 after 100 days of exposure to the test brines at 150°C and a gamma dose rate of 10 Gy/h

Brine	Corrosion rate (µm/a)
1	173.0
2	208.3
3	21.0

brines 1 and 2: $MgCl_2$-rich; brine 3: NaCl-rich

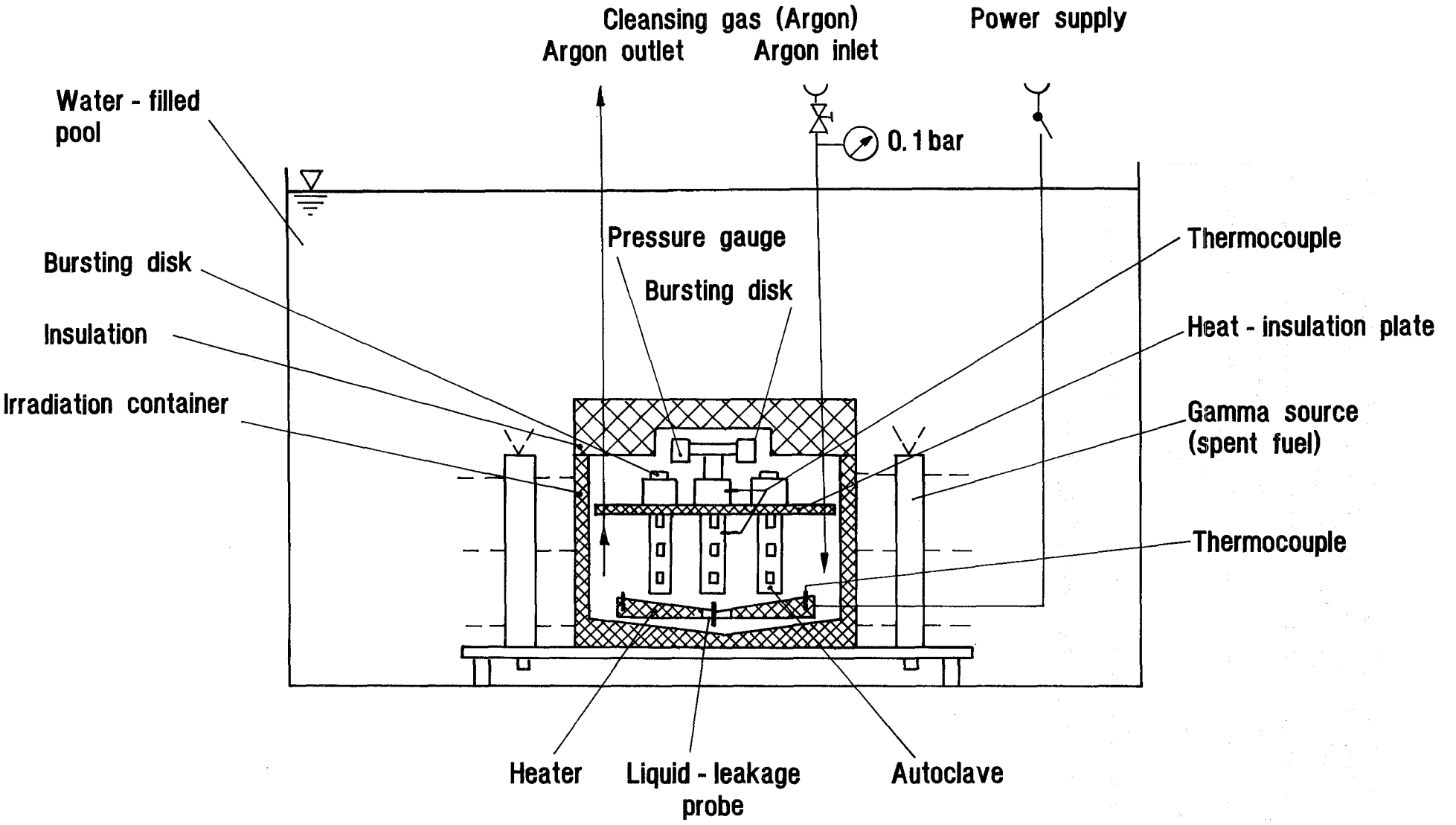

Fig. 1: Schematic of irradiation-corrosion test facility

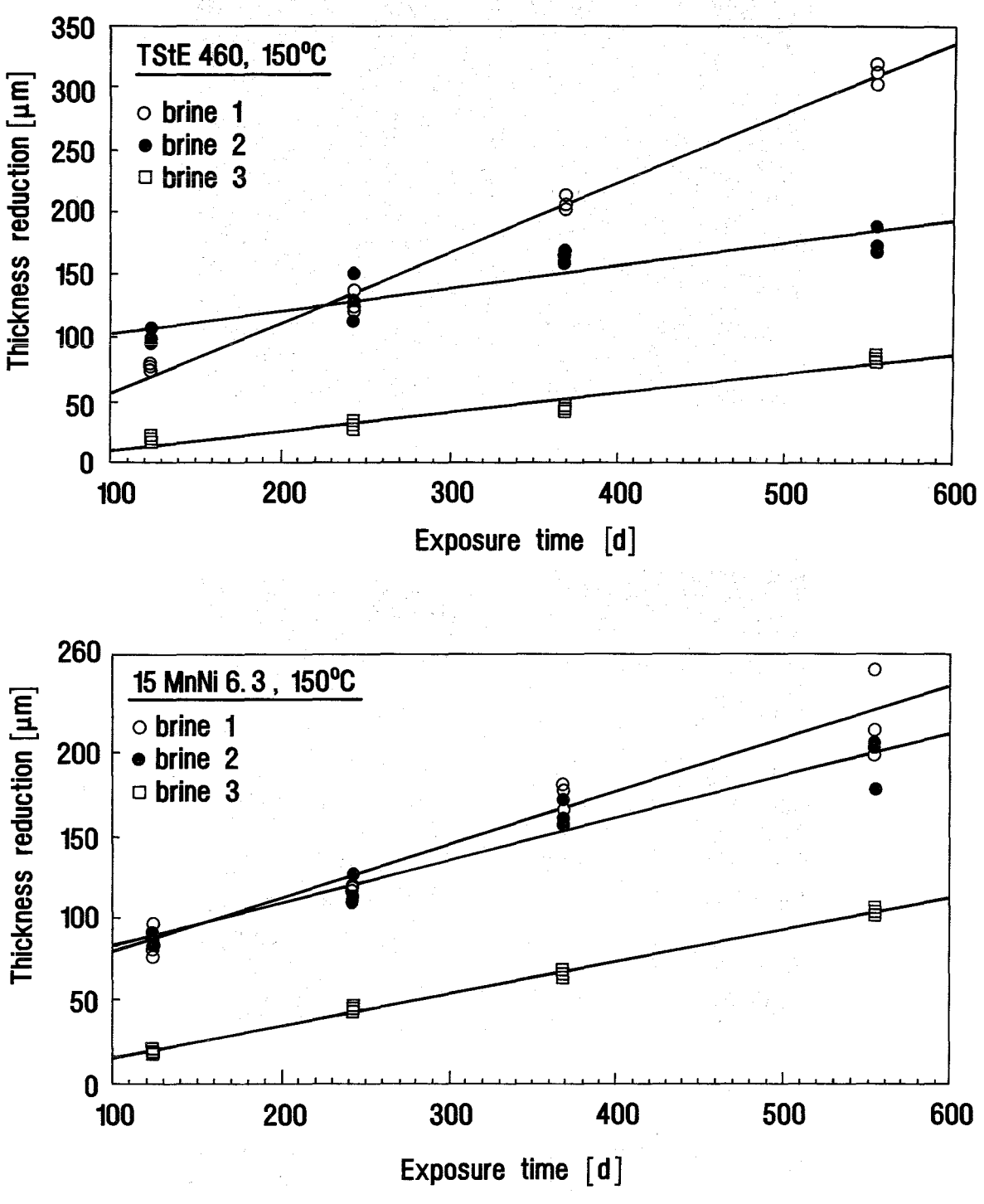

Fig.2: Thickness reduction of the steels TStE 460 and 15 MnNi 6.3 in salt brines at 150°C

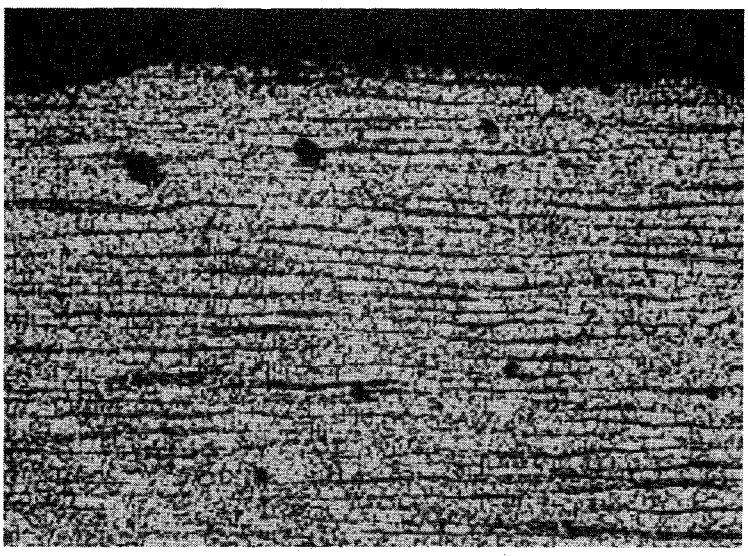

TSt E 460 X 100

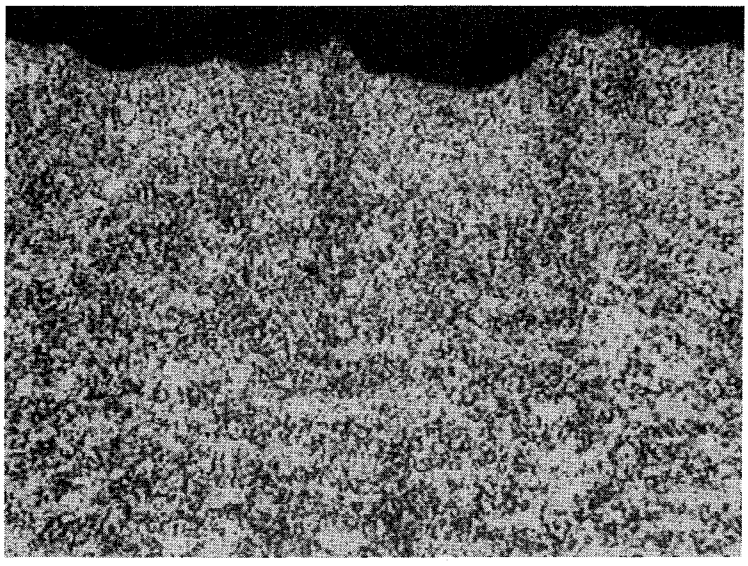

15 MnNi 6.3 X 50

Fig.3: Optical micrographs of the unwelded steels TSt E 460 and 15 MnNi 6.3 after an 18-month exposure to brine 1 (Q-brine) at 150°C

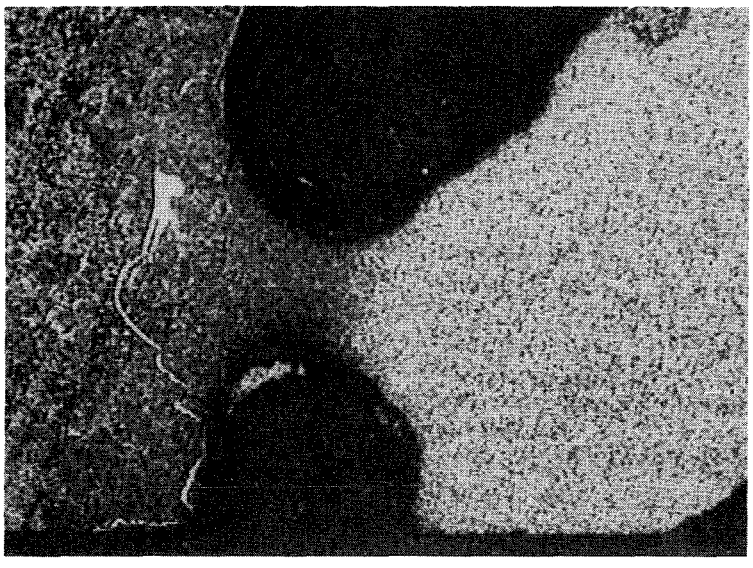

TSt E 460 X 20

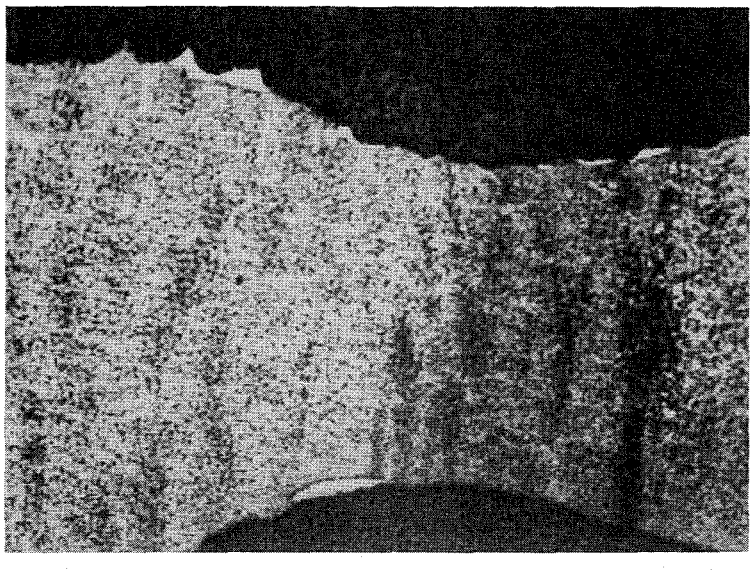

15 MnNi 6.3 X 20

Fig.4: Optical micrographs of the submerged arc welded steels TSt E 460 and 15 MnNi 6.3 after an 18-month exposure to brine 1 (Q-brine) at 150°C

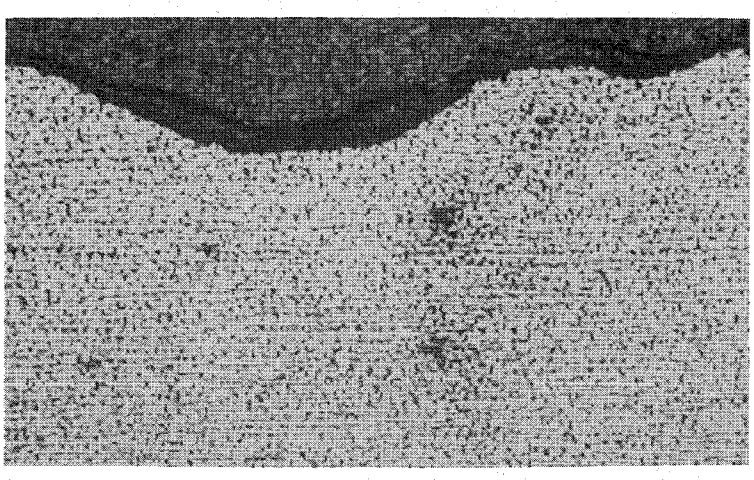

Brine 1 ($MgCl_2$-rich) X 100

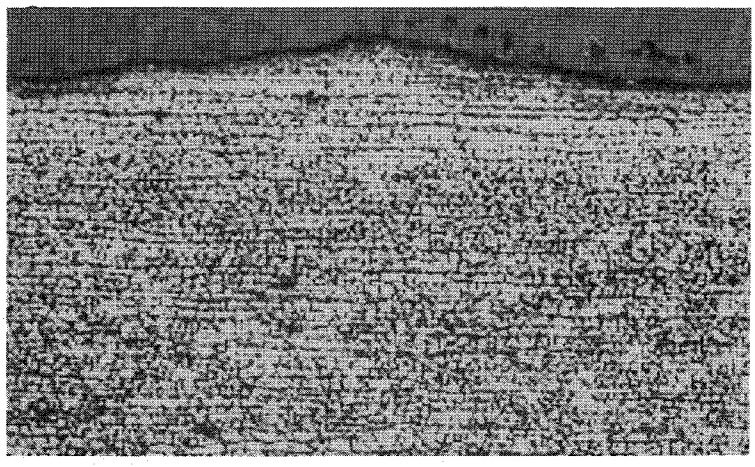

Brine 2 ($MgCl_2$-rich) X 100

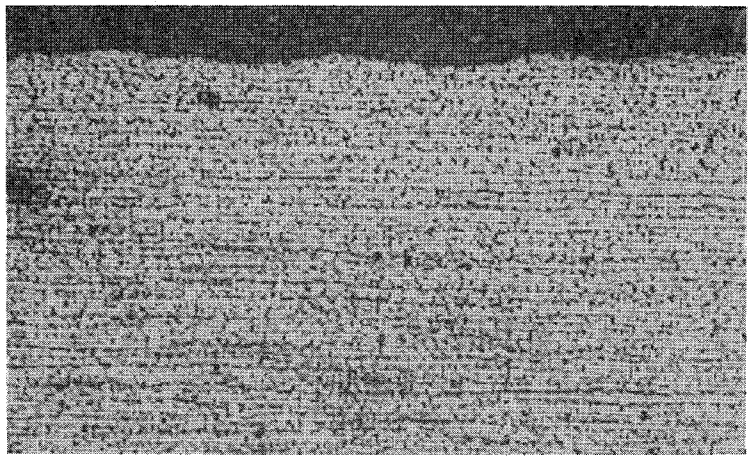

Brine 3 (NaCl-rich) X 100

Fig.5: Optical micrographs of the steel TSt E 355 after 100 days exposure to brines at 150°C and 10 Gy/h

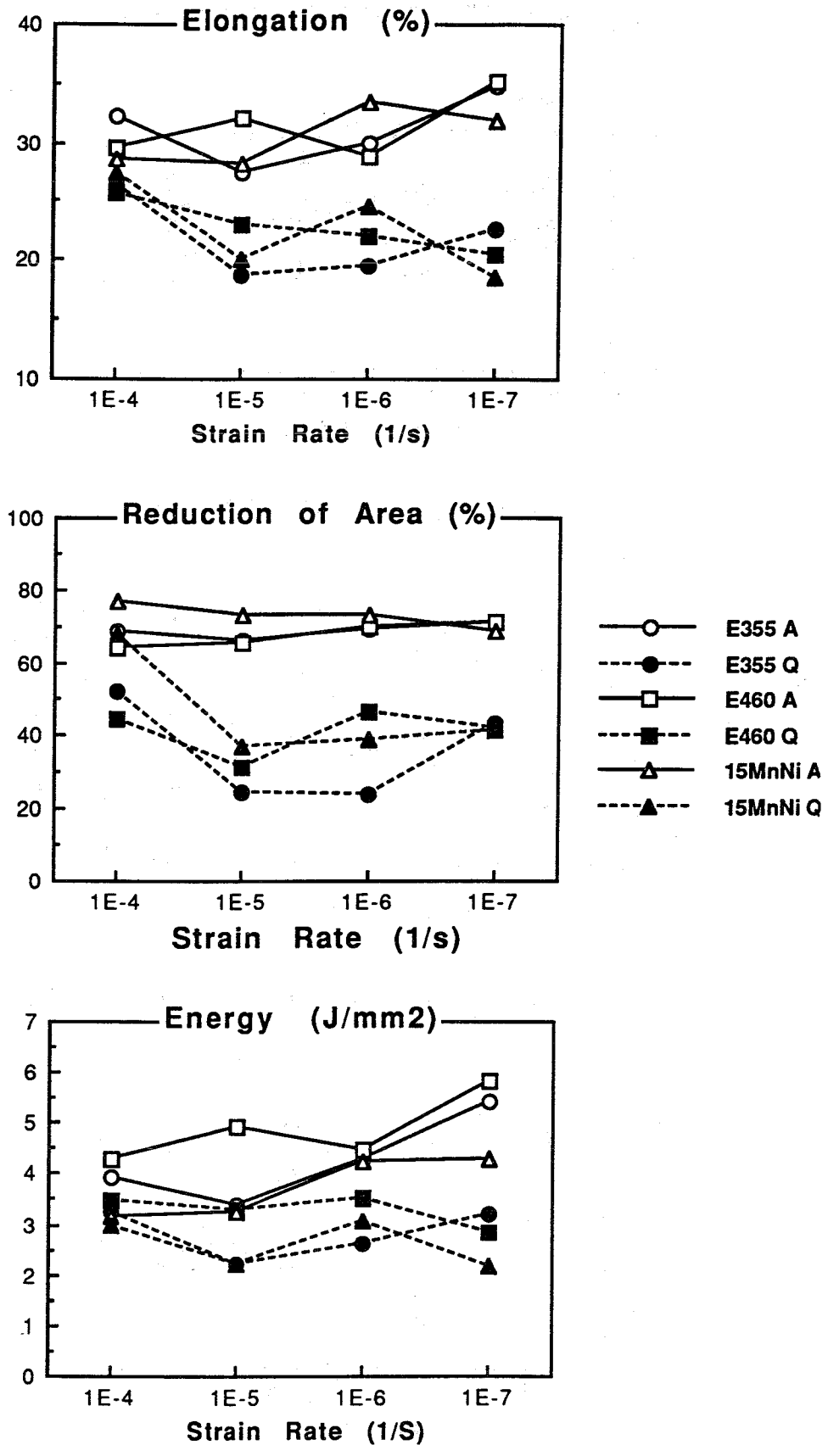

Fig.6: Elongation, reduction of area and energy versus strain rate for the steels TSt E 355, TSt E 460 and 15 MnNi 6.3 tested at 170°C and 13 MPa in argon and Q-brine

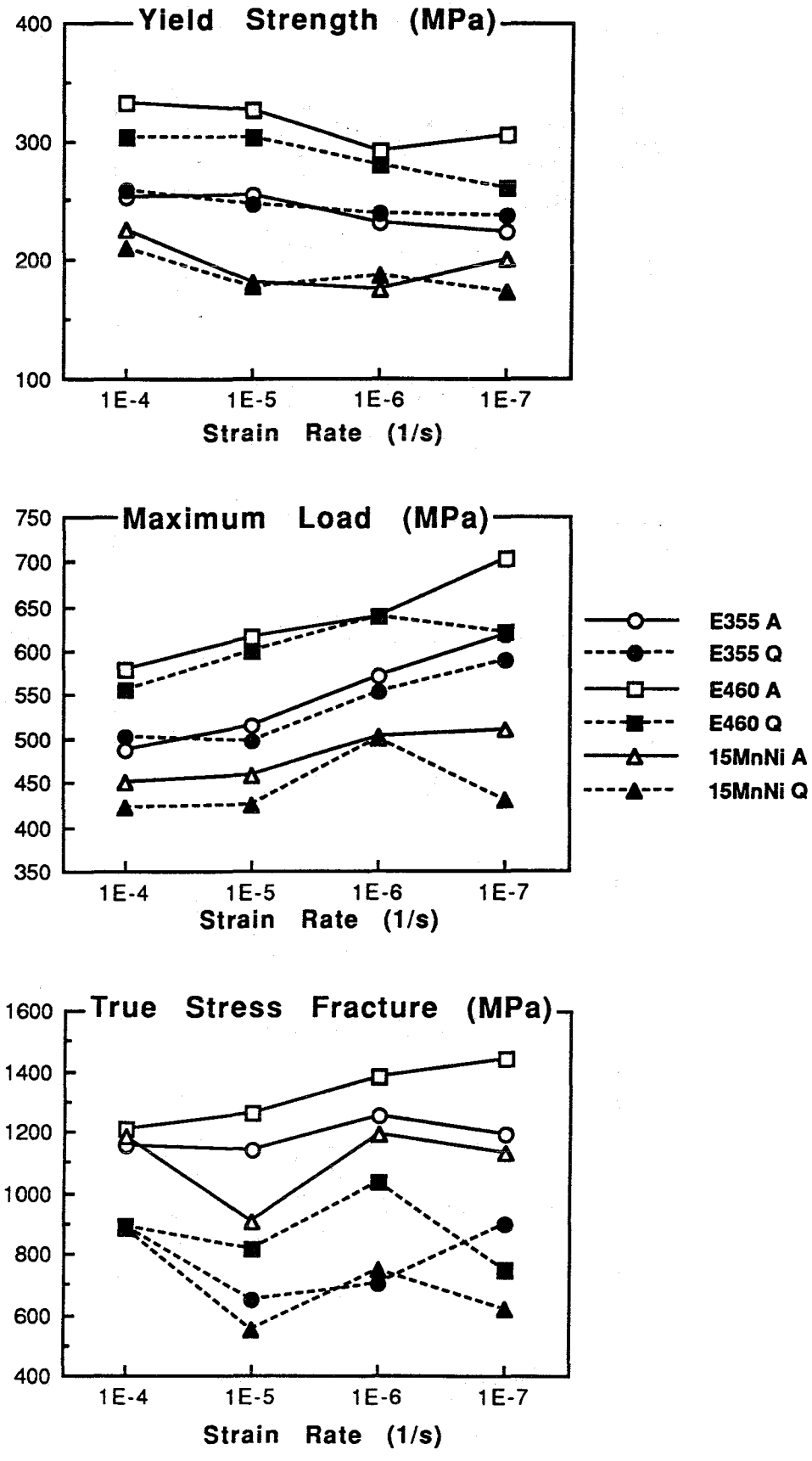

Fig.7: Yield strength, maximum load and true stress fracture versus strain rate for the steels TSt E 355, TSt E 460 and 15 MnNi 6.3 tested at 170°C and 13 MPa in argon and Q-brine

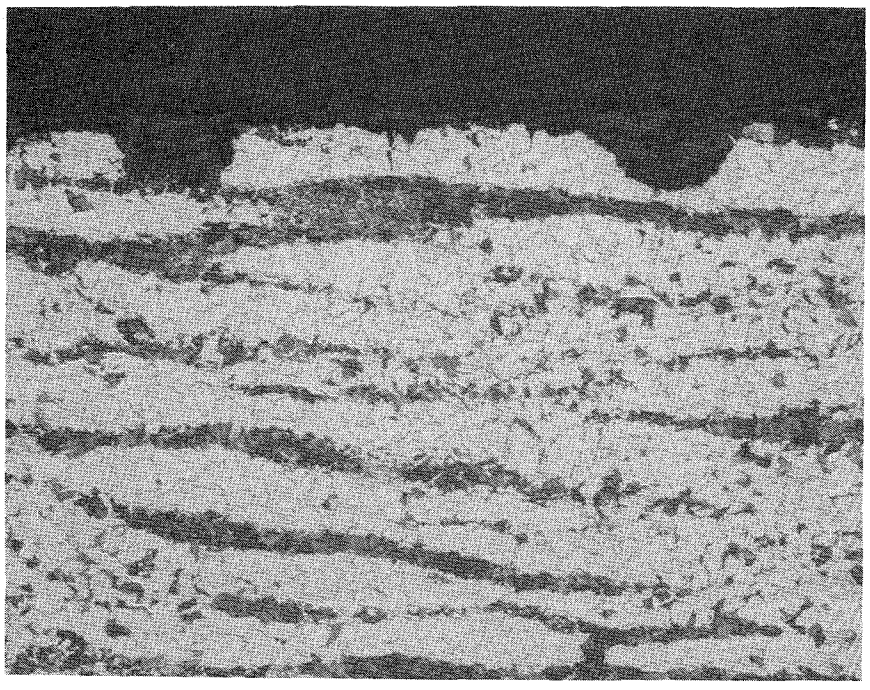

TSt E 355 X 200

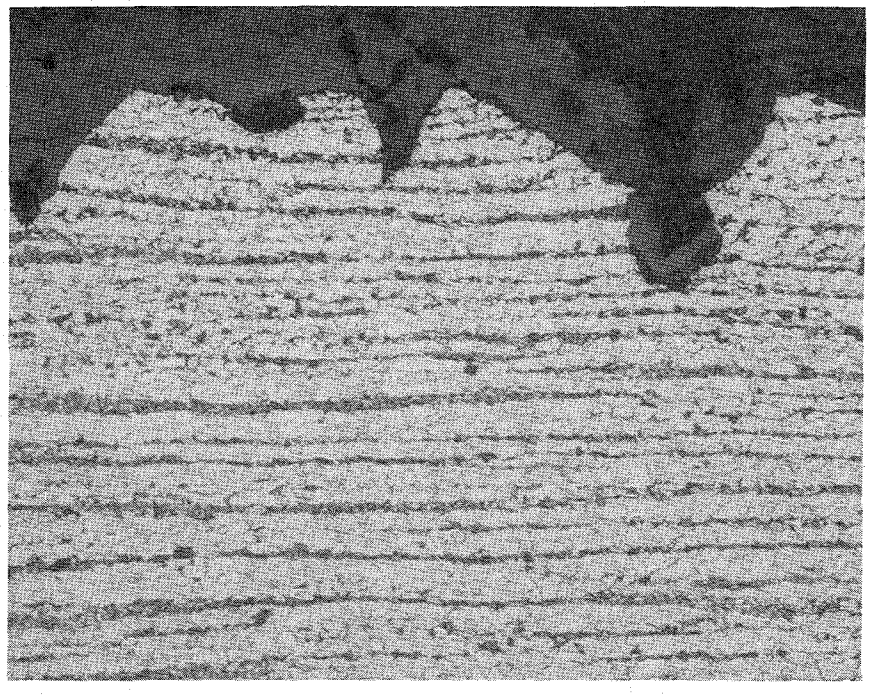

TSt E 460 X 200

Fig.8: Optical micrographs of the steels TSt E 355 and TSt E 460 tested in Q-brine at 170°C, 13 MPa and $10^{-5} s^{-1}$

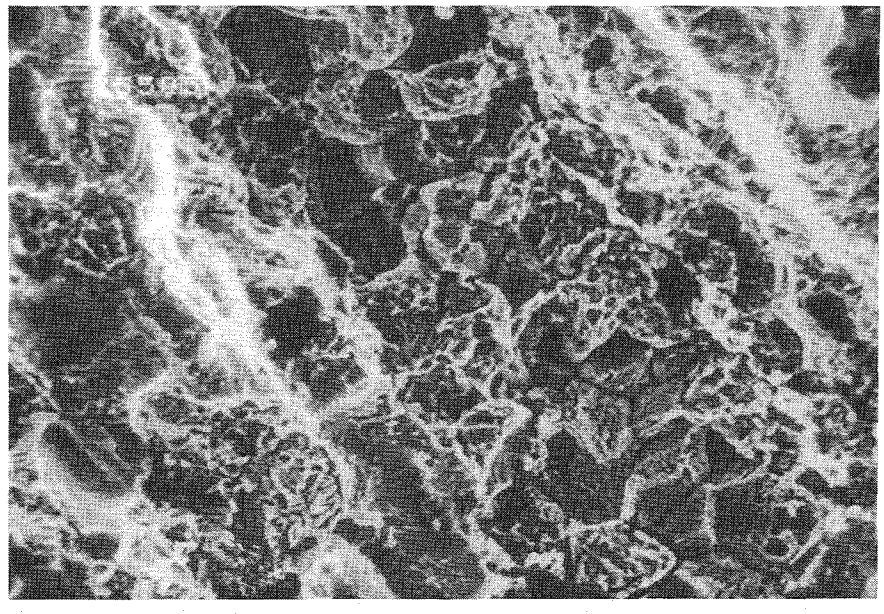

TSt E 355, $10^{-5}s^{-1}$ X 500

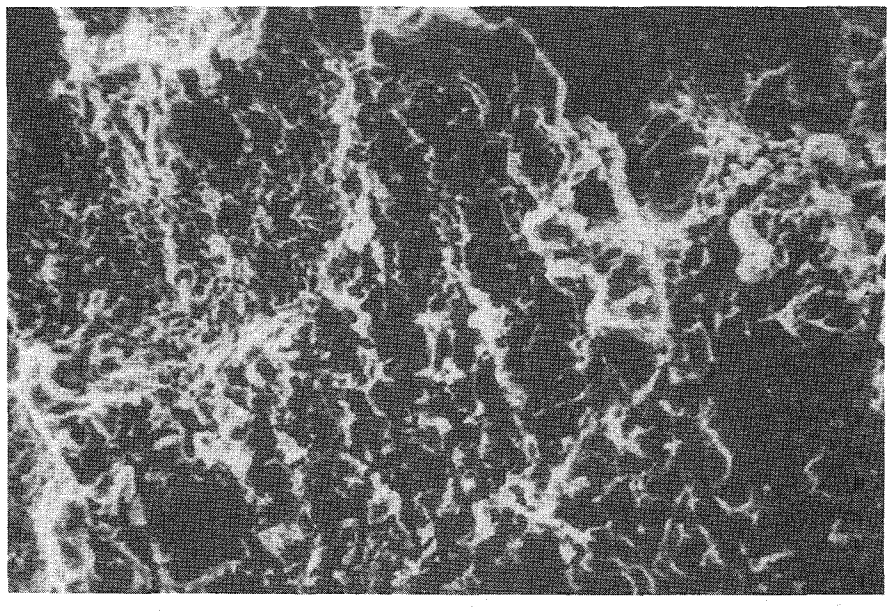

TSt E 460, $10^{-7}s^{-1}$ X 750

Fig.9: SEM micrographs of the steels TStE 355 and TSt E 460 tested in Q-brine at 170°C, 13 MPa and strain rates of $10^{-5}s^{-1}$ and $10^{-7}s^{-1}$, respectively

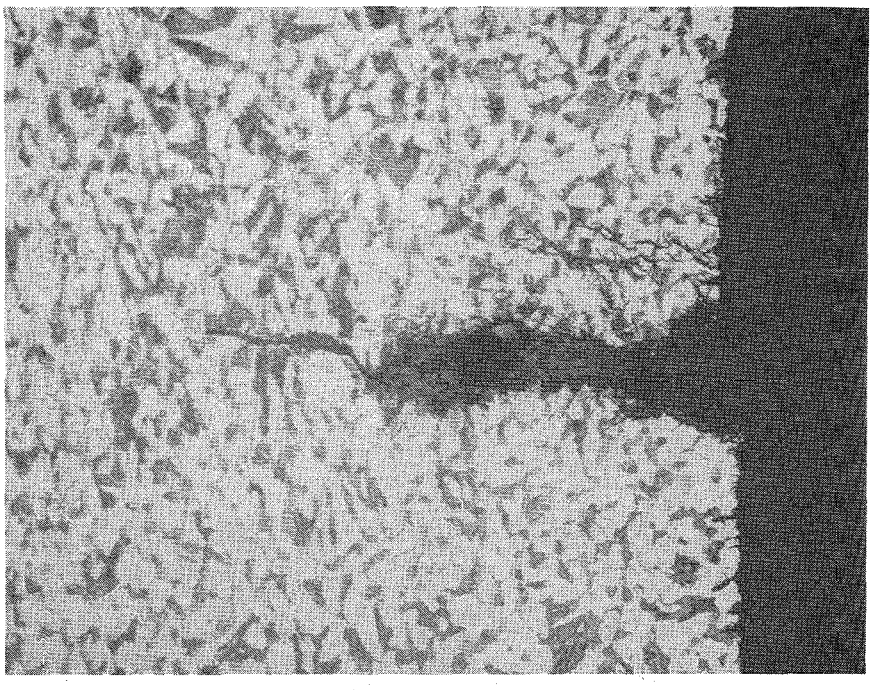

X 200

Fig.10: Optical micrograph of the steel 15 MnNi 6.3 tested in Q-brine at 170°C, 13 MPa and $10^{-5}s^{-1}$

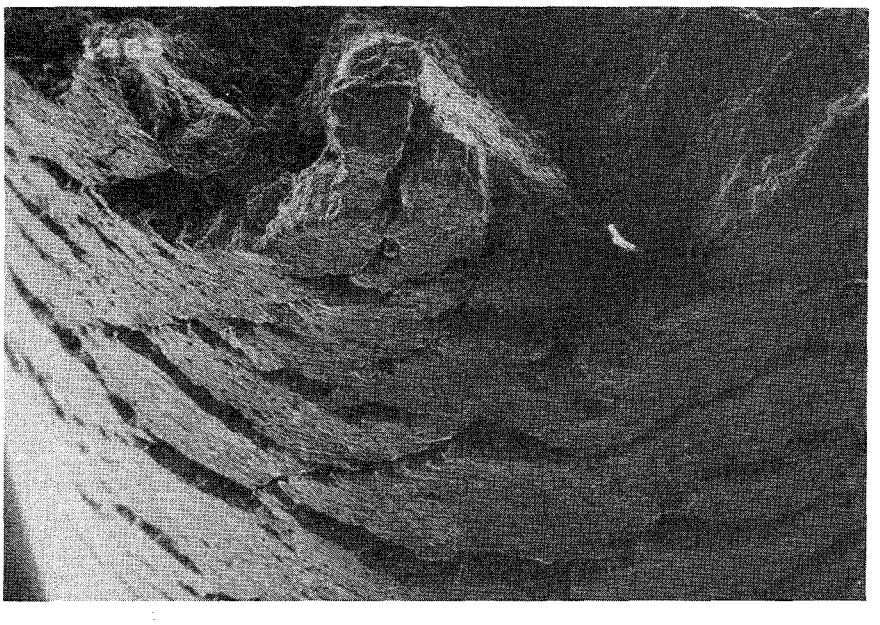

X 20

Fig.11: SEM micrograph of the steel 15 MnNi 6.3 tested in Q-brine at 170°C, 13 MPa and $10^{-5}s^{-1}$

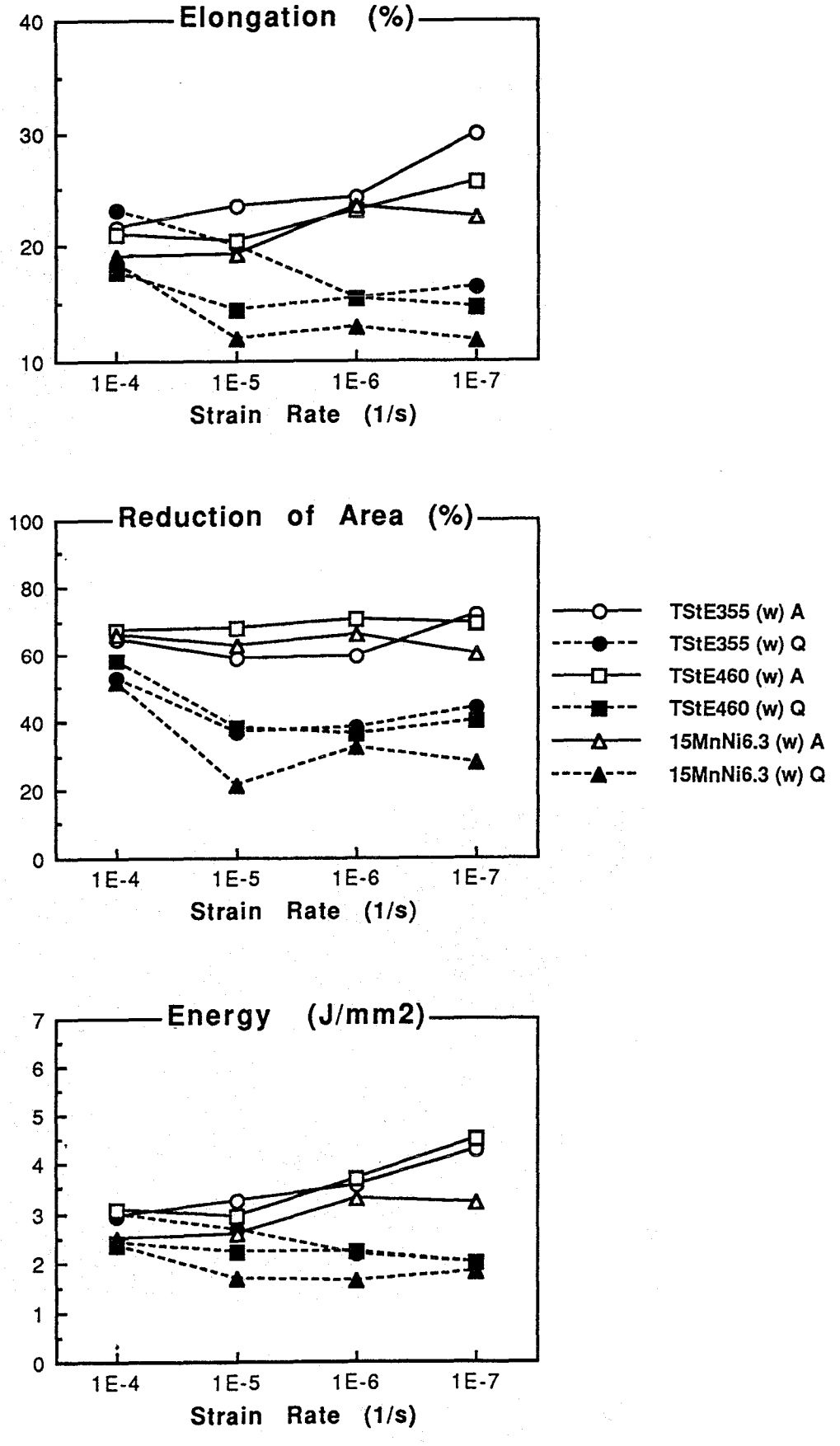

Fig.12: Elongation, reduction of area and energy versus strain rate for the MAG welded steels TSt E 355, TSt E 460 and 15 MnNi 6.3 tested at 170°C and 13 MPa in argon and Q-brine

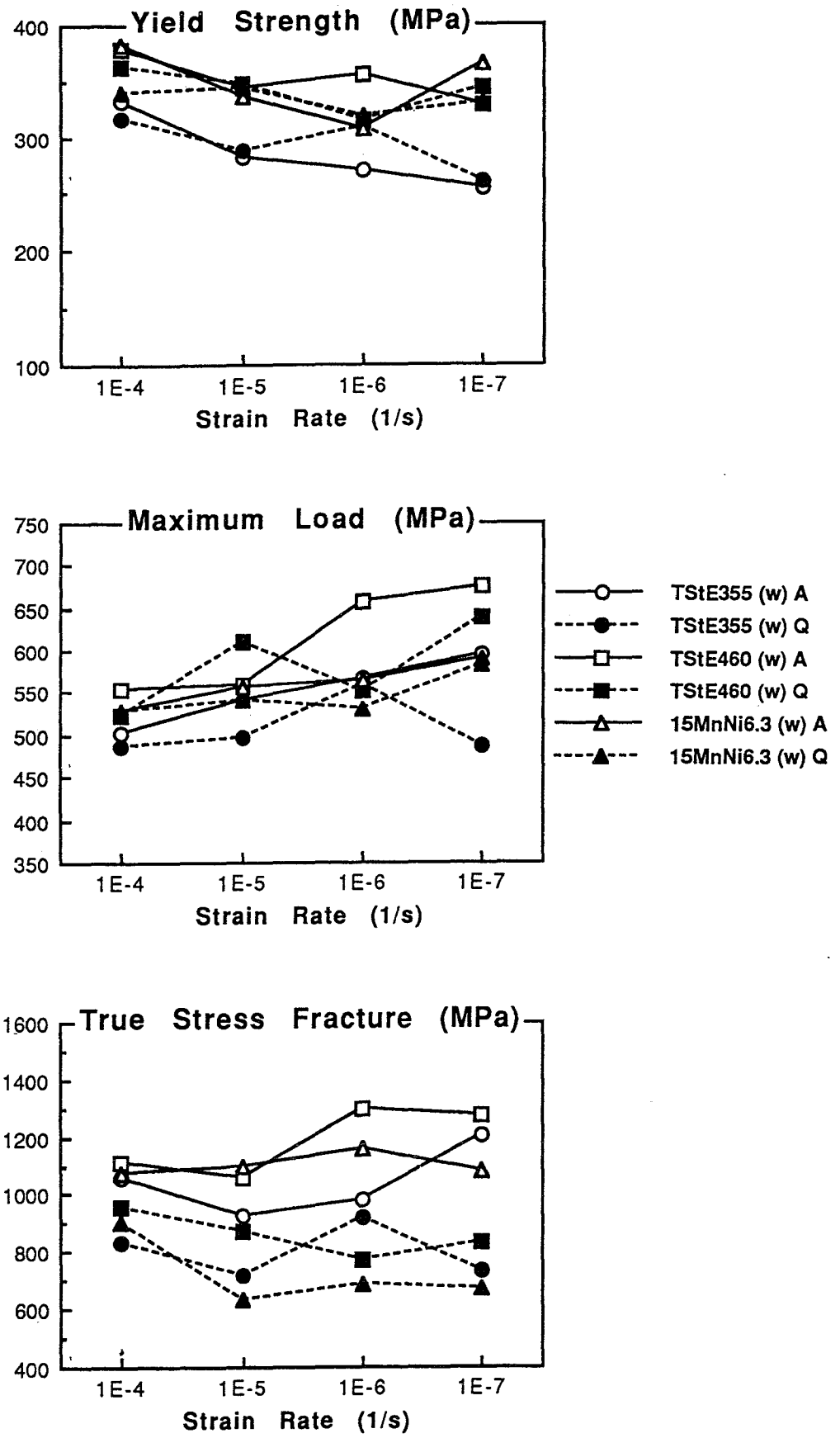

Fig.13: Yield strength, maximum load and true stress fracture versus strain rate for the MAG welded steels TSt E 355, TSt E 460 and 15 MnNi 6.3 tested at 170°C and 13 MPa in argon and Q-brine